Low-energy bremsstrahlung photon in relativistic nucleon + nucleon collisions

Taesoo Song[1,*] and Pierre Moreau[2]

[1]Institut für Theoretische Physik, Universität Gießen, D-35392 Gießen, Germany
[2]Institute for Theoretical Physics, Johann Wolfgang Goethe Universität, D-60438 Frankfurt am Main, Germany

(Received 19 October 2018; published 19 December 2018)

We study the production of bremsstrahlung photons in relativistic nucleon + nucleon collisions by introducing a deceleration time of electromagnetic currents. It is found that the bremsstrahlung photon spectrum at low energy does not depend on the deceleration time, but solely on the amount of reduced electromagnetic current in collision. On the other hand, the photon spectrum becomes soft with increasing deceleration time. We also find that the bremsstrahlung photon spectrum in $p + n$ collisions is quite different from that in $p + p$ collisions at low energy.

DOI: 10.1103/PhysRevD.98.116007

I. INTRODUCTION

Relativistic heavy-ion collisions are presently the unique way to produce extremely hot and dense nuclear matter in the laboratory and to study the properties of such matter. There are several kinds of probe particles through which one can investigate the properties, and the electromagnetic probe is one of them. The electromagnetic probe is distinguished from other particles in a couple of respects. First of all, it has no color charge and interacts only through electromagnetic coupling that is much weaker than strong coupling, so it gets out of the nuclear matter without any further interactions after it is produced. Second, it is continuously produced from initial hard scattering until after freeze-out in relativistic heavy-ion collisions.

Photons produced in relativistic heavy-ion collisions are classified into three groups according to production stage. The first group of photons is produced through initial hard scattering, which can be obtained by rescaling the photon spectrum in nucleon + nucleon collisions with the number of binary collisions. Then, the produced nuclear matter emits thermal photons both in quark-gluon plasma and in the hadron gas phase. The third group of photons is produced through the electromagnetic decay of hadrons mostly after the freeze-out. The first two groups of photons are called "direct photons," and the last group are called "indirect photons."

Nucleon + nucleon collisions serve as reference experiments to study the nuclear matter produced in heavy-ion collisions, because the latter are hardly able to produce sizable matter, unless the collision happens near Large Hadron Collider (LHC) energies. For example, when direct photons in a $p + p$ collision are subtracted from those in a heavy-ion collision with the number of binary collisions multiplied, the leftovers are interpreted as thermal photons [1]. In this respect, studying photon production in nucleon + nucleon collisions is the first step toward studying the nuclear matter produced in relativistic heavy-ion collisions.

In the microscopic view, direct photons are produced in nucleon + nucleon collisions through the scattering of quarks and antiquarks composing the nucleons, for example, $q + \bar{q} \to g + \gamma$, $q(\bar{q}) + g \to q(\bar{q}) + \gamma$, and so on. These elementary scattering cross sections are convoluted with parton distribution functions of nucleons. However, this perturbative quantum chromodynamics (pQCD) approach with the factorization formula is reliable only for large-energy momentum transfer—in other words, for the production of high-energy photons.

Another source of direct photons is the bremsstrahlung, which is the electromagnetic radiation from decelerated charged particles. *Brems* means "to brake" from the German word *bremsen*, and *strahlung* means "radiation." Microscopically, the bremsstrahlung photon is produced through the parton scatterings: $q + \bar{q} \to q + \bar{q} + \gamma$ or $q + q(g) \to q + q(g) + \gamma$ or $\bar{q} + \bar{q}(g) \to \bar{q} + \bar{q}(g) + \gamma$. However, if the energy of the emitted photon is low, it looks like $N + N \to N + N + \gamma$ in low-energy collisions or $N + N \to X + X' + \gamma$ in high-energy collisions, where X and X' represent wounded nucleons which still carry electromagnetic currents in the beam direction.

If the collision energy is extremely large, two nucleons pass through each other, and the stopping or deceleration of electromagnetic currents can be reduced to a one-dimensional problem. Since the nucleon is not a pointlike particle but a composite particle, and abundant particles are

*taesoo.song@theo.physik.uni-giessen.de

produced in high-energy collisions, this stopping should be described by a smooth function of time. In this Letter, we model the production of low-energy bremsstrahlung photons in relativistic nucleon + nucleon collisions, introducing a finite stopping time of electromagnetic currents.

We first describe in Sec. II the stopping of charged particles from the simplest case to more sophisticated ones step by step, and we take into account the structure of the nucleon in Sec. III. After that, the stopping or deceleration of charged particles takes place by collisions in Sec. IV, and the results are applied to relativistic nucleon + nucleon collisions in Sec. V. Finally, a summary is given in Sec. VI, and several useful Fourier transformations are presented in the Appendix.

II. STOPPING OF CHARGED PARTICLES

A. No stopping

The momentum distribution of radiated photons from decelerated charged particles is expressed as [2–4]

$$\omega\frac{dN}{d^3\mathbf{k}}=\frac{1}{2(2\pi)^3}\sum_\lambda|j(\omega,\mathbf{k})\cdot\epsilon^\lambda(\omega,\mathbf{k})|^2, \tag{1}$$

where ω and $\mathbf{k}$ are the photon energy and momentum, $j(\omega,\mathbf{k})$ is the electromagnetic current, and $\epsilon^\lambda(\omega,\mathbf{k})$ is the polarization vector of emitted photons, with λ being the polarization state.

As a warm-up, we consider a particle with electric charge Q and velocity v without stopping or deceleration. The electromagnetic current is then given by

$$\mathbf{j}(t,\mathbf{r})=Qv\delta(z-vt)\delta(x)\delta(y)\mathbf{e_z}, \tag{2}$$

where $\mathbf{e_z}$ is the unit vector in the z direction. The position of the charged particle Fourier-transformed,

$$\mathbf{j}(t,\mathbf{k})=\int d^3\mathbf{r}\mathbf{j}(t,\mathbf{r})e^{i\mathbf{r}\cdot\mathbf{k}}=Qve^{ik_zvt}\mathbf{e_z}, \tag{3}$$

and t-transformed into ω, is

$$\begin{aligned}\int dt\mathbf{j}(t,\mathbf{k})e^{-i\omega t}&=Qv\int dte^{i(k_zv-\omega)t}\mathbf{e_z}\\&=2\pi Qv\delta(k_zv-\omega)\mathbf{e_z}.\end{aligned} \tag{4}$$

Substituting Eq. (4) into Eq. (1), the spectrum of radiated photons is given by

$$\begin{aligned}\omega\frac{dN}{d^3\mathbf{k}}&=\frac{1}{4\pi}\sum_\lambda\{Qv\epsilon_z^\lambda\delta(k_zv-\omega)\}^2\\&=\frac{1}{4\pi}\sum_\lambda\{Qv\epsilon_z^\lambda\delta[\omega(v\cos\theta-1)]\}^2,\end{aligned} \tag{5}$$

where we use the Coulomb gauge ($\epsilon^0=0$) and θ is the angle of $\mathbf{k}$ with respect to $\mathbf{e_z}$. Since a charged particle in nature always has a nonvanishing mass, it cannot reach the speed of light ($v<1$). Therefore,

$$\omega\frac{dN}{d^3\mathbf{k}}=0. \tag{6}$$

Now, we deal with the stopping of a charged particle from the simplest case to more sophisticated ones step by step.

B. Instant stopping

In the simplest case, a particle with the constant velocity v and the electric charge Q instantly stops at $(t,\mathbf{r})=(0,0)$. The current is described by

$$\mathbf{j}(t,\mathbf{r})=Qv\delta(z-vt)\delta(x)\delta(y)\theta(-t)\mathbf{e_z}, \tag{7}$$

which is the same as Eq. (2) except for the step function $\theta(-t)$. Carrying out Fourier transformations,

$$\mathbf{j}(t,\mathbf{k})=\int d^3\mathbf{r}\mathbf{j}(t,\mathbf{r})e^{i\mathbf{r}\cdot\mathbf{k}}=Qv\theta(-t)e^{ik_zvt}\mathbf{e_z}, \tag{8}$$

and then

$$\begin{aligned}\int dt\mathbf{j}(t,\mathbf{k})e^{-i\omega t}&=Qv\int dt\theta(-t)e^{i(k_zv-\omega)t}\mathbf{e_z}\\&=Qv\left\{\pi\delta(\omega-k_zv)+\frac{i}{\omega-k_zv}\right\}\mathbf{e_z}\end{aligned} \tag{9}$$

by using Eq. (A5) and the relation

$$\theta(-t)=\frac{1}{2}\{1-\mathrm{sgn}(t)\}, \tag{10}$$

where $\mathrm{sgn}(t)$ is the signum function. Dropping off the delta function in Eq. (9), the spectrum of emitted photons is given by

$$\omega\frac{dN}{d^3\mathbf{k}}=\frac{1}{2(2\pi)^3}\sum_\lambda\left(\frac{Qv\epsilon_z^\lambda}{\omega-k_zv}\right)^2, \tag{11}$$

which is in covariant form [5,6]

$$\omega\frac{dN}{d^3\mathbf{k}}=\frac{1}{2(2\pi)^3}\sum_\lambda Q^2\left(\frac{p\cdot\epsilon^\lambda}{p\cdot k}\right)^2, \tag{12}$$

where p is the four-momentum of the charged particle.

Now, we turn to the polarization vector of the photon. Suppose the photon momentum and a polarization vector are expressed, respectively, as

$$\vec{k} = (0, \quad 0, \quad k),$$
$$\vec{\epsilon}^{1} = (\cos\varphi, \quad \sin\varphi, \quad 0), \tag{13}$$

where φ is the polarization angle. Rotating $\vec{k}$ by an angle θ around the y axis and then by an angle ϕ around the z axis, we get

$$\vec{k}' = \begin{pmatrix} \cos\phi & -\sin\phi & 0 \\ \sin\phi & \cos\phi & 0 \\ 0 & 0 & 1 \end{pmatrix} \begin{pmatrix} \cos\theta & 0 & \sin\theta \\ 0 & 1 & 0 \\ -\sin\theta & 0 & \cos\theta \end{pmatrix} \begin{pmatrix} 0 \\ 0 \\ k \end{pmatrix} = \begin{pmatrix} k\sin\theta\cos\phi \\ k\sin\theta\sin\phi \\ k\cos\theta \end{pmatrix},$$
$$\vec{\epsilon}^{1\prime} = \begin{pmatrix} \cos\phi & -\sin\phi & 0 \\ \sin\phi & \cos\phi & 0 \\ 0 & 0 & 1 \end{pmatrix} \begin{pmatrix} \cos\theta & 0 & \sin\theta \\ 0 & 1 & 0 \\ -\sin\theta & 0 & \cos\theta \end{pmatrix} \begin{pmatrix} \cos\varphi \\ \sin\varphi \\ 0 \end{pmatrix} = \begin{pmatrix} \cos\theta\cos\phi\cos\varphi - \sin\phi\sin\varphi \\ \cos\theta\sin\phi\cos\varphi + \cos\phi\sin\varphi \\ -\sin\theta\cos\varphi \end{pmatrix}. \tag{14}$$

Since $\epsilon^1 \cdot \mathbf{e_z} = -\sin\theta\cos\varphi$, the average of $(\epsilon^1 \cdot \mathbf{e_z})^2$ in Eq. (11) over φ turns to

$$\frac{1}{2\pi}\int_0^{2\pi} d\varphi (\epsilon^1 \cdot \mathbf{e_z})^2 = \frac{1}{2}\sin^2\theta, \tag{15}$$

and

$$\frac{1}{2\pi}\sum_{\lambda=1,2}\int_0^{2\pi} d\varphi (\epsilon^\lambda \cdot \mathbf{e_z})^2 = \sin^2\theta, \tag{16}$$

because ϵ_2 has the same contribution as ϵ_1. The same result is obtained by using the relation

$$\sum_{\lambda=1,2} \epsilon_i^\lambda \epsilon_j^{\lambda *} = \delta_{ij} - \hat{k}_i \hat{k}_j, \tag{17}$$

where $\hat{k}_i = k_i/|\mathbf{k}|$. Therefore, at midrapidity ($\sin\theta = 1$),

$$\left.\frac{dN}{d^2k_T dy}\right|_{y=0} = \frac{1}{2(2\pi)^3}\left(\frac{Qv}{\omega}\right)^2, \tag{18}$$

where $\sum_\lambda (\epsilon^\lambda \cdot \mathbf{e_z})^2$ is substituted with 1, as will be applied throughout this Letter.

C. Smooth stopping

Next, we deal with smooth stopping by using a hyperbolic tangent function instead of a step function in Eq. (7):

$$\mathbf{j}(t, \mathbf{r}) = Qv\delta(z - vt)\delta(x)\delta(y)\frac{1 - \tanh(at)}{2}\mathbf{e_z}, \tag{19}$$

where for simplicity we assume that the particle keeps its initial velocity but the electric charge evaporates with time and a controls evaporation time.

The electromagnetic current is modified by Fourier transformations into

$$\mathbf{j}(t, \mathbf{k}) = Qv\frac{1 - \tanh(at)}{2}e^{ik_z vt}\mathbf{e_z}, \tag{20}$$

and

$$\int dt \mathbf{j}(t, \mathbf{k}) e^{-i\omega t} = Qv\int dt \frac{1 - \tanh(at)}{2} e^{i(k_z v - \omega)t}\mathbf{e_z} = Qv\left\{\pi\delta(\omega - k_z v) + \frac{\pi i}{2a}\mathrm{csch}\left(\frac{\pi(\omega - k_z v)}{2a}\right)\right\}\mathbf{e_z} \tag{21}$$

by using Eq. (A9). Ignoring the unphysical pole at $\omega = k_z v$,

$$\omega\left.\frac{dN}{d^3k}\right|_{y=0} = \frac{1}{2(2\pi)^3}\left(\frac{\pi Qv}{2a}\right)^2 \mathrm{csch}^2\left(\frac{\pi\omega}{2a}\right). \tag{22}$$

We can find that Eq. (22) converges into Eq. (18) in the limit of $a \to \infty$, because

$$\lim_{x\to 0}\mathrm{csch}x = \frac{1}{x}. \tag{23}$$

The upper panel of Fig. 1 shows the normalized electromagnetic current as a function of rescaled time. Since we use a hyperbolic tangent function, the deceleration of charged particles starts very early. However, we can define the effective stopping time as $2/a$, during which electromagnetic current decreases from 88% to 12%.

We show in the lower panel the photon spectra at midrapidity for various stopping times of a proton whose initial energy is 100 GeV. $\alpha = e^2/(4\pi)$ is taken to be $1/137$. Though the proton is not a pointlike particle, its detailed structure is ignored for simplicity. The figure clearly shows that as the stopping time increases, the photon spectrum becomes soft. One interesting point is that the photon spectrum at very low frequencies does not depend on the stopping time. We will explain the reason for this in the following section.

D. Stepwise stopping

Now, we describe the smooth stopping by discretizing the process. As with the first trial, we assume that a charged particle changes its velocity from v_i to v_f at $(t, z) = (0, 0)$. Then the electromagnetic current is expressed as

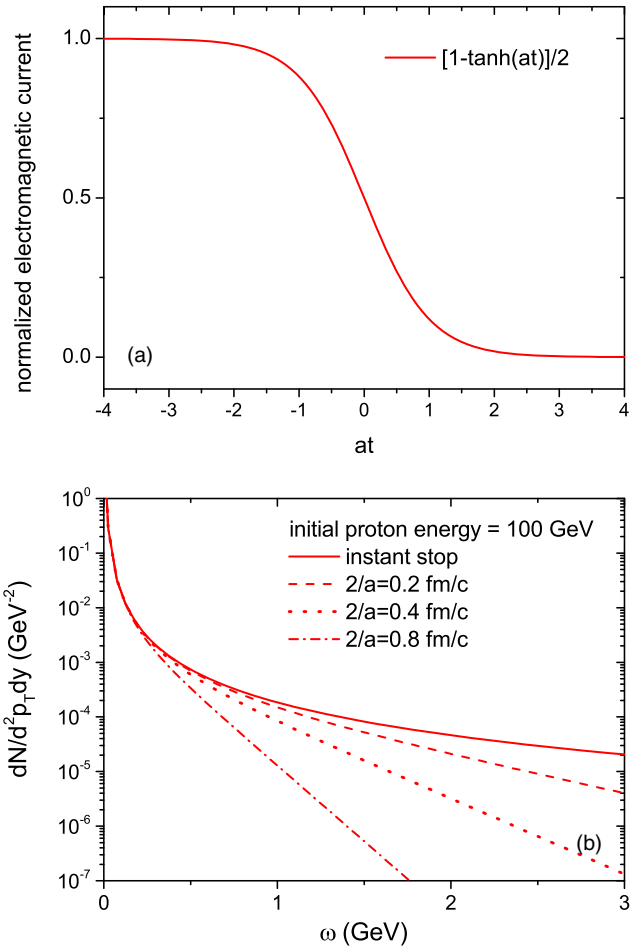

FIG. 1. (a) Normalized electromagnetic current as a function of rescaled time. (b) Photon spectra at midrapidity for various stopping times of the proton, whose initial energy is 100 GeV.

$$\mathbf{j}(t,\mathbf{r}) = Qv(t)\delta(z - v(t)t)\delta(x)\delta(y)\mathbf{e_z}, \tag{24}$$

where $v(t) = v_i\theta(-t) + v_f\theta(t)$. After Fourier transformations, the current turns to

$$\mathbf{j}(t,\mathbf{k}) = \int d^3\mathbf{r}\mathbf{j}(t,\mathbf{r})e^{i\mathbf{r}\cdot\mathbf{k}} = Qv(t)e^{ik_z v(t)t}\mathbf{e_z}, \tag{25}$$

and

$$\begin{aligned}\int dt\mathbf{j}(t,\mathbf{k})e^{-i\omega t} &= Q\left\{v_i\int dt\theta(-t)e^{i(k_z v_i-\omega)t}\right.\\ &\quad\left.+ v_f\int dt\theta(t)e^{i(k_z v_f-\omega)t}\right\}\mathbf{e_z}\\ &= Q\left\{\frac{iv_i}{\omega - k_z v_i} - \frac{iv_f}{\omega - k_z v_f}\right\}\mathbf{e_z},\end{aligned} \tag{26}$$

where we have removed insignificant delta functions and will do so from here on. We can find that Eq. (26) is equivalent to Eq. (9) in the case of $v_f = 0$.

Now, we suppose the charged particle is decelerated in two steps—that is, the velocity changes from v_i to v_m at $t = -T/2$, and then to v_f at $t = T/2$:

$$v(t) = v_i\theta(-t - T/2) + v_m\mathrm{rect}_T(t) + v_f\theta(t - T/2), \tag{27}$$

with $\mathrm{rect}_T(t)$ being the box function defined in Eq. (A6), and the position of charged particle is

$$\begin{aligned}z(t) &= \int dtv(t) = v_m t \quad \text{for } |t| \le T/2,\\ &= v_m T/2 + v_f(t - T/2) \quad \text{for } t > T/2,\\ &= -v_m T/2 + v_i(t + T/2) \quad \text{for } t < -T/2.\end{aligned} \tag{28}$$

Carrying out Fourier transformations,

$$\mathbf{j}(t,\mathbf{k}) = \int d^3\mathbf{r}\mathbf{j}(t,\mathbf{r})e^{i\mathbf{r}\cdot\mathbf{k}} = Qv(t)e^{ik_z z(t)}\mathbf{e_z}, \tag{29}$$

and

$$\begin{aligned}&\int dt\mathbf{j}(t,\mathbf{k})e^{-i\omega t}\\ &= Qv_i e^{i(\omega - k_z v_m)T/2}\int dt'\theta(-t')e^{i(k_z v_i-\omega)t'}\mathbf{e_z}\\ &\quad + Qv_m\int dt\mathrm{rect}_T(t)e^{i(k_z v_m-\omega)t}\mathbf{e_z}\\ &\quad + Qv_f e^{i(k_z v_m-\omega)T/2}\int dt''\theta(t'')e^{i(k_z v_f-\omega)t''}\mathbf{e_z},\end{aligned} \tag{30}$$

where $t' = t + T/2$ and $t'' = t - T/2$. By using Eq. (A5),

$$\begin{aligned}\mathbf{j}(\omega,\mathbf{k}) = iQ\left[\left(\frac{v_i}{\omega - k_z v_i} - \frac{v_m}{\omega - k_z v_m}\right)e^{i(\omega - k_z v_m)T/2}\right.\\ \left.+\left(\frac{v_m}{\omega - k_z v_m} - \frac{v_f}{\omega - k_z v_f}\right)e^{-i(\omega - k_z v_m)T/2}\right]\mathbf{e_z}.\end{aligned} \tag{31}$$

If the intermediate time interval T is extremely short, Eq. (31) returns to Eq. (26):

$$\lim_{T\to 0}\mathbf{j}(\omega,\mathbf{k}) = iQ\left(\frac{v_i}{\omega - k_z v_i} - \frac{v_f}{\omega - k_z v_f}\right)\mathbf{e_z}. \tag{32}$$

We can interpret Eq. (31) as follows: The first and second terms represent the first and second photon emissions at $t = -T/2$ and $t = T/2$, respectively, and the two exponential functions show their phases. Therefore, Eq. (31) can be generalized to N-photon emissions [7]:

$$\mathbf{j}(w,\mathbf{k}) = iQ\sum_{i=1}^{N}\left(\frac{v_{i-}}{w - k_z v_{i-}} - \frac{v_{i+}}{w - k_z v_{i+}}\right)e^{-i\phi_{i1}}\mathbf{e_z}, \tag{33}$$

where v_{i-} and v_{i+} are, respectively, the velocities of charged particles before and after the ith photon emission, with a ϕ_{i1} phase difference between the first and the ith photons, which is given by

$$\phi_{11} = 0, \tag{34}$$

$$\phi_{i1} = \sum_{j=1}^{i-1} (\omega - k_z v_{j+}) \Delta t_j^{j+1} = \sum_{j=1}^{i-1} \omega (1 - v_{j+} \cos\theta) \Delta t_j^{j+1}, \tag{35}$$

with Δt_j^{j+1} being the time interval between the jth and the $(j+1)$th photon emissions. If the photon energy ω is small enough, we may ignore the phase differences in Eq. (33), and the electromagnetic current turns out to be

$$\lim_{\omega\to 0} \mathbf{j}(\omega, \mathbf{k}) = iQ \sum_{i=1}^{N} \left(\frac{v_{i-}}{\omega - k_z v_{i-}} - \frac{v_{i+}}{\omega - k_z v_{i+}} \right) \mathbf{e_z} = iQ \left(\frac{v_i}{\omega - k_z v_i} - \frac{v_f}{\omega - k_z v_f} \right) \mathbf{e_z}, \tag{36}$$

which is equivalent to Eq. (26). It explains why the photon spectrum near $\omega = 0$ does not change for various stopping times in Fig. 1(b). Low-energy photons cannot provide the information of short timescales.

Now, we apply the stepwise method to the previous section, where a charged particle moves with a constant velocity but electric charge evaporates with time. Supposing the electric charge changes from Q_i to Q_f at $t = 0$, the electromagnetic current is given by

$$\mathbf{j}(t, \mathbf{r}) = Q(t) v \delta(z - vt) \delta(x) \delta(y) \mathbf{e_z}, \tag{37}$$

where

$$Q(t) = Q_i \theta(-t) + Q_f \theta(t), \tag{38}$$

and after Fourier transformations it turns to

$$\mathbf{j}(\omega, \mathbf{k}) = \int dt d^3\mathbf{r} \mathbf{j}(t, \mathbf{r}) e^{i(\mathbf{k}\cdot\mathbf{r} - \omega t)} = i \frac{(Q_i - Q_f) v}{\omega - k_z v} \mathbf{e_z}. \tag{39}$$

Next, suppose the particle changes its electric charge from Q_i to Q_m at $t = -T/2$, and then from Q_m to Q_f at $t = T/2$:

$$Q(t) = Q_i \theta(-t - T/2) + Q_m \mathrm{rect}_T(t) + Q_f \theta(t - T/2). \tag{40}$$

Then, the Fourier-transformed current is given by

$$\mathbf{j}(\omega, \mathbf{k}) = \int dt d^3\mathbf{r} \mathbf{j}(t, \mathbf{r}) e^{i(\mathbf{k}\cdot\mathbf{r} - \omega t)} = iv \left\{ \frac{Q_i - Q_m}{\omega - k_z v} e^{-i(k_z v - \omega) T/2} + \frac{Q_m - Q_f}{\omega - k_z v} e^{i(k_z v - \omega) T/2} \right\} \mathbf{e_z}. \tag{41}$$

Compared to Eq. (39), this is nothing but the summation of two currents with phase terms. Therefore, we can generalize it to N-photon emissions as before:

$$\mathbf{j}(\omega, \mathbf{k}) = iv \sum_{i=1}^{N} \frac{Q_{i-} - Q_{i+}}{\omega - k_z v} e^{-i\phi_{i1}} \mathbf{e_z}, \tag{42}$$

where Q_{i-} and Q_{i+} are, respectively, particle charges before and after the ith photon emission with a ϕ_{i1} phase difference between the first and the ith photons, which is given by

$$\phi_{11} = 0, \tag{43}$$

$$\phi_{i1} = \sum_{j=1}^{i-1} (\omega - k_z v) \Delta t_j^{j+1} = \sum_{j=1}^{i-1} \omega (1 - v \cos\theta) \Delta t_j^{j+1}, \tag{44}$$

with Δt_j^{j+1} being the time interval between the jth photon emission and the $(j+1)$th photon emission. We point out that at midrapidity ($\cos\theta = 0$), Eqs. (33) and (42) are expressed in unified form:

$$\mathbf{j}(\omega, \mathbf{k}) = i \sum_{i=1}^{N} \frac{j_{i-} - j_{i+}}{\omega} e^{-i\phi_{i1}} \mathbf{e_z}, \tag{45}$$

where $j_{i-} \equiv Q_{i-} v_{i-}$ and $j_{i+} \equiv Q_{i+} v_{i+}$ are, respectively, the electromagnetic currents before and after the ith photon emission with the phase difference

$$\phi_{11} = 0, \qquad \phi_{i1} = \sum_{j=1}^{i-1} \omega \Delta t_j^{j+1}. \tag{46}$$

In other words, bremsstrahlung photons from a decelerated charged particle and those from a particle whose electric

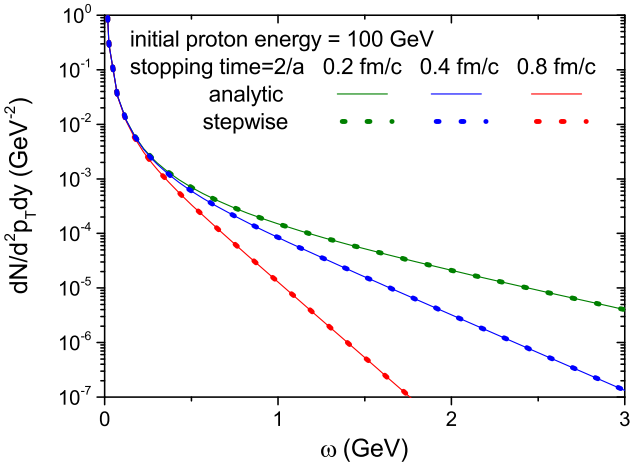

FIG. 2. Photon spectra at midrapidity from proton stopping with an initial energy of 100 GeV between analytic solution in Eq. (22) and the results from the stepwise method.

charge evaporates are indistinguishable at midrapidity, if the particle velocity and the evaporation speed are the same.

Figure 2 compares photon spectra at midrapidity from proton stopping with an initial energy of 100 GeV between the analytic solution in Eq. (22) and the results from the stepwise method. We can see that the stepwise method reproduces the analytic solution.

III. CONSIDERATION OF NUCLEON STRUCTURE

The proton is not a pointlike particle but a composite particle made up of at least three valence quarks. In this section, we substitute the proton with three valence quarks which are randomly distributed in a sphere with radius R. Since the photon spectra from charge evaporation and from deceleration are the same at midrapidity, we take the former case for simplicity. The electromagnetic current from three comoving valence quarks is given by

$$\mathbf{j}(t,\mathbf{r}) = \sum_{i=1\sim3} Q_i v \delta(z-vt)\delta(x-x_i)\delta(y-y_i) \times \frac{1-\tanh(at)}{2}\mathbf{e_z}, \tag{47}$$

where Q_i is the electric charge of valence quark i, and $z_i = 0$ at $t = 0$ is assumed from the Lorentz contraction in ultrarelativistic collisions. We also assume that x_i and y_i do not change with time, even after collision. The current is transformed in momentum space as follows:

$$\mathbf{j}(t,\mathbf{k}) = \int d^3\mathbf{r}\mathbf{j}(t,\mathbf{r})e^{i\mathbf{r}\cdot\mathbf{k}} = \sum_{i=1\sim3} Q_i v \frac{1-\tanh(at)}{2} e^{i(k_x x_i + k_y y_i + k_z vt)}\mathbf{e_z} \tag{48}$$

and

$$\mathbf{j}(\omega,\mathbf{k}) = \int dt \mathbf{j}(\mathbf{k},t)e^{-i\omega t} = i\frac{\pi v}{2a}\operatorname{csch}\left(\frac{\pi(\omega-k_z v)}{2a}\right)\sum_{i=1-3} Q_i e^{i(k_x x_i + k_y y_i)}\mathbf{e_z}. \tag{49}$$

Therefore, we can find the relation

$$\omega\frac{dN}{d^3k}\bigg|_{\text{with structure}} = \omega\frac{dN}{d^3k}\bigg|_{\text{pointlike}} \times \left|\sum_{i=1-3} q_i e^{i(k_x x_i + k_y y_i)}\right|^2, \tag{50}$$

where $q_i = Q_i/(\sum_{j=1-3} Q_j)$. Rotating the coordinate system such that $(k_x, k_y) \to (k_T, 0)$, the correction factor is simplified into

$$\left|\sum_{i=1-3} q_i e^{i(k_x x_i + k_y y_i)}\right|^2 = \sum_{i,j=1-3} q_i q_j e^{ik_T(x_i - x_j)} = \sum_{i,j=1-3} q_i q_j \cos\{k_T(x_i - x_j)\}, \tag{51}$$

where sine term in the last equation vanishes. In the limit $k_T \to 0$, the correction factor turns to unity:

$$\lim_{k_T\to0}\left|\sum_{i=1-3} q_i e^{i(k_x x_i + k_y y_i)}\right|^2 = \sum_{i,j=1-3} q_i q_j = 1. \tag{52}$$

This means again that a photon with a very small frequency does not provide the information of the detailed structure of a charged particle. We can calculate the expectation value of the cosine function in the case $x_i \neq x_j$ as follows:

$$\begin{aligned}
&\langle\cos\{k_T(x_i - x_j)\}\rangle|_{x_i\neq x_j} \\
&= \frac{1}{(4/3\pi R^3)^2}\int dV_i dV_j \\
&\quad\times\{\cos(k_T x_i)\cos(k_T x_j) + \sin(k_T x_i)\sin(k_T x_j)\} \\
&= \frac{1}{(2/3R^3)^2}\left\{\int_0^R dr_i r_i^2 \int_{-1}^1 d\cos\theta_i \cos(k_T r_i\cos\theta_i)\right\}^2 \\
&= \frac{9}{(k_T R)^6}\{-k_T R\cos(k_T R) + \sin(k_T R)\}^2,
\end{aligned} \tag{53}$$

where θ_i is the angle between $\mathbf{k_T}$ and $\mathbf{r_i}$, and finally

$$\begin{aligned}
&\left|\sum_{i=1-3} q_i e^{i(k_x x_i + k_y y_i)}\right|^2 \\
&= \sum_{i=1-3} q_i^2 + \frac{9}{(k_T R)^6}\{-k_T R\cos(k_T R) + \sin(k_T R)\}^2 \\
&\quad\times\sum_{i\neq j} q_i q_j.
\end{aligned} \tag{54}$$

Figure 3 shows the correction factors for proton structure as a function of the transverse momentum of the photon with the proton radius R taken to be 1 fm. In order to get an insight, we use three different combinations of quarks (uud, $uudu\bar{u}$, $uudd\bar{d}$) for the proton. The magenta line shows Eq. (53), which starts with 1.0 at $k_T = 0$ GeV and then almost vanishes before $k_T = 1$ GeV. It explains the behavior of correction factors in Fig. 3. For example, supposing that the proton is composed of $uudu\bar{u}$, the correction factor at small k_T

$$\left(\frac{2}{3}+\frac{2}{3}-\frac{1}{3}+\frac{2}{3}-\frac{2}{3}\right)^2 = 1, \tag{55}$$

and at large k_T

$$\left(\frac{2}{3}\right)^2+\left(\frac{2}{3}\right)^2+\left(-\frac{1}{3}\right)^2+\left(\frac{2}{3}\right)^2+\left(-\frac{2}{3}\right)^2 = \frac{17}{9}, \tag{56}$$

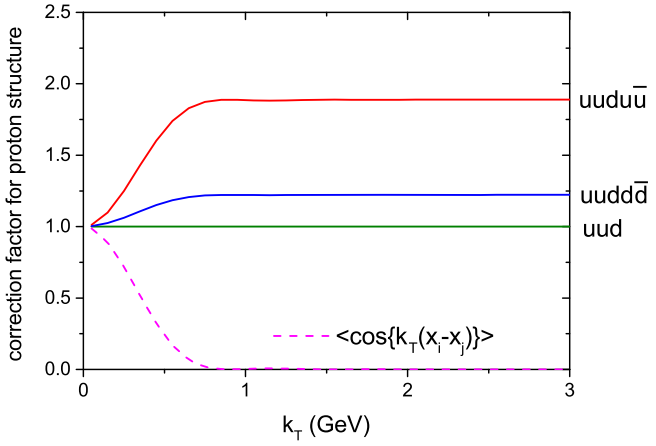

FIG. 3. Correction factors for proton structure as a function of the transverse momentum of photons for different combinations of quarks (uud, $uudu\bar{u}$, $uudd\bar{d}$). The proton radius R is taken to be 1 fm, and the magenta line shows Eq. (53).

which means that the individual quark is not seen at small k_T but is seen at large k_T. In other words, the coherent photon smoothly changes into an incoherent photon as photon energy increases. However, if only valence quarks are considered (uud), there is no difference between coherent and incoherent photons, because the correction factor

$$\left(\frac{2}{3}+\frac{2}{3}-\frac{1}{3}\right)^2=1 \tag{57}$$

at small k_T is equivalent to

$$\left(\frac{2}{3}\right)^2+\left(\frac{2}{3}\right)^2+\left(-\frac{1}{3}\right)^2=1 \tag{58}$$

at large k_T. We may consider the proton as the combination of $uudu\bar{u}$ or $uudd\bar{d}$, taking $u\bar{u}$ or $d\bar{d}$ for the sea-quark pair. In this case, however, the sea quark and sea antiquark are not located independently in the nucleon but are strongly correlated in space, so that their effect will appear at much larger photon energy.

IV. STOPPING IN COLLISION

In this section, we describe the stopping of two particles in collision. For simplicity, two particles move in opposite directions with the same velocity and electric charges, Q_1 and Q_2, and evaporate with time:

$$\mathbf{j}(t,\mathbf{r})=v\delta(y)\frac{1-\tanh(at)}{2}\{Q_1\delta(x-b/2)\delta(z-vt) - Q_2\delta(x+b/2)\delta(z+vt)\}\mathbf{e_z}, \tag{59}$$

where b is the impact parameter [8]. Taking Fourier transformations,

$$\mathbf{j}(t,\mathbf{k})=\int d^3\mathbf{r}\mathbf{j}(t,\mathbf{r})e^{i\mathbf{r}\cdot\mathbf{k}}=v\frac{1-\tanh(at)}{2} \times\{Q_1e^{i(k_zvt+k_xb/2)}-Q_2e^{-i(k_zvt+k_xb/2)}\}\mathbf{e_z}, \tag{60}$$

and

$$\mathbf{j}(\omega,\mathbf{k})=\int dt\mathbf{j}(t,\mathbf{k})e^{-i\omega t} =i\frac{\pi v}{2a}\left\{Q_1\mathrm{csch}\left(\frac{\pi(\omega-k_zv)}{2a}\right)e^{ik_xb/2} - Q_2\mathrm{csch}\left(\frac{\pi(\omega+k_zv)}{2a}\right)e^{-ik_xb/2}\right\}\mathbf{e_z}. \tag{61}$$

The only difference in Eq. (61) from Eq. (21) is two phase terms, which is ascribed to the separation of two currents in the x direction. It is straightforward to prove that the photon spectrum from the evaporation of two electric charges is identical to that from the deceleration of two charged particles at midrapidity as shown in the previous section. By using Eq. (61), the photon spectrum at midrapidity ($k_z=0$) from the collision turns out to be

$$\left.\frac{dN}{d^2k_Tdy}\right|_{y=0}=\frac{1}{2(2\pi)^3}\sum_\lambda|\mathbf{j}(\omega,\mathbf{k})\cdot\boldsymbol{\epsilon}^\lambda(\omega,\mathbf{k})|^2 =\frac{1}{16\pi}\left(\frac{v}{2a}\right)^2\mathrm{csch}^2\left(\frac{\pi\omega}{2a}\right)\left\{(Q_1-Q_2)^2 + 4Q_1Q_2\sin^2\left(\frac{k_xb}{2}\right)\right\}. \tag{62}$$

Equation (62) applied to $p+n$ collisions ($Q_1=e$, $Q_2=0$) is

$$\left.\frac{dN}{d^2k_Tdy}\right|_{y=0}=\frac{1}{16\pi}\left(\frac{j}{2a}\right)^2\mathrm{csch}^2\left(\frac{\pi\omega}{2a}\right), \tag{63}$$

and applied to $p+p$ collisions ($Q_1=Q_2=e$) is

$$\left.\frac{dN}{d^2k_Tdy}\right|_{y=0}=\frac{1}{4\pi}\left(\frac{j}{2a}\right)^2\mathrm{csch}^2\left(\frac{\pi\omega}{2a}\right)\sin^2\left(\frac{k_xb}{2}\right), \tag{64}$$

where $j=Q_iv_i$. We note that if the impact parameter $b=0$ in a $p+p$ collision, the photon spectrum vanishes at midrapidity, though this hardly happens in reality. If electric charges do not completely stop, which is usual in high-energy collisions, the electromagnetic currents j in Eqs. (63) and (64) are substituted for by $\Delta j=Q_iv_i-Q_fv_f$, the change of electromagnetic current.

Equation (62) can be applied to heavy-ion collisions, assuming that the nucleus is a pointlike particle [8]. In this case, Q_1 and Q_2 are the electric charges of the participants of the projectile and target nuclei, respectively, and b is the

mean transverse distance between the participants of the projectile nucleus and those of the target nucleus.

Equation (61) is reexpressed in terms of the valence quark, substituting Q_1 and Q_2 into $\sum_j Q_j e^{i\mathbf{k}\cdot\mathbf{r}_j}$ as in Eq. (49):

$$\begin{aligned}&\mathbf{j}(\omega,\mathbf{k}_T,k_z=0)\\&=i\frac{\pi v}{2a}\mathrm{csch}\left(\frac{\pi\omega}{2a}\right)\\&\quad\times\sum_i(Q_{1i}e^{ik_T\cdot(\mathbf{r}_{1i}+\mathbf{b}/2)}-Q_{2i}e^{ik_T\cdot(\mathbf{r}_{2i}-\mathbf{b}/2)})\mathbf{e_z},\end{aligned}\tag{65}$$

where $Q_{1i}(Q_{2i})$ and $\mathbf{r}_{1i}(\mathbf{r}_{2i})$ are, respectively, the electric charge and the transverse position from the center of nucleon 1(2) of quark i, which composes nucleon 1(2). Following the previous section, it is straightforward to calculate the photon spectrum:

$$\begin{aligned}\left.\frac{dN}{d^2k_Tdy}\right|_{y=0}&=\frac{1}{16\pi}\left(\frac{v}{2a}\right)^2\mathrm{csch}^2\left(\frac{\pi\omega}{2a}\right)\\&\quad\times\Bigg[\sum_{i,j}Q_{1i}Q_{1j}\cos\{k_T(x_{1i}-x_{1j})\}\\&\quad+\sum_{i,j}Q_{2i}Q_{2j}\cos\{k_T(x_{2i}-x_{2j})\}\\&\quad-2\sum_{i,j}Q_{1i}Q_{2j}\cos\{k_T(x_{1i}-x_{2j}+b\cos\phi)\}\Bigg],\end{aligned}\tag{66}$$

where the coordinate system is rotated such that k_T is parallel to $\mathbf{e_x}$ and ϕ is the angle between b and k_T. Assuming that quarks are randomly distributed in nucleons whose radius is R,

$$\begin{aligned}\left.\frac{dN}{d^2k_Tdy}\right|_{y=0}&=\frac{1}{16\pi}\left(\frac{v}{2a}\right)^2\mathrm{csch}^2\left(\frac{\pi\omega}{2a}\right)\\&\quad\times\Bigg[\sum_i(Q_{1i}^2+Q_{2i}^2)\\&\quad+\frac{9}{(k_TR)^6}\{-k_TR\cos(k_TR)+\sin(k_TR)\}^2\\&\quad\times\Bigg\{\sum_{i\neq j}(Q_{1i}Q_{1j}+Q_{2i}Q_{2j})\\&\quad-2\cos(k_Tb\cos\phi)\sum_{ij}Q_{1i}Q_{2j}\Bigg\}\Bigg],\end{aligned}\tag{67}$$

which converges to Eq. (62) in the limit $R\to 0$.

In the picture of pQCD, only one parton in the nucleon interacts with one parton from the other nucleon. However, if a valence quark gets out of the nucleon by scattering, the remaining two valence quarks cannot proceed without interaction, because they are not color singlet any more. They should somehow be involved in the scattering. Though the stopping or deceleration of three valence quarks might be different from each other, we can simply take their average.

We note that Eq. (67) can be applied to nucleus-nucleus collision with $Q_{1i}(Q_{2i})$ and R being the electric charges of nucleon i in nucleus 1(2) and the nucleus radius, respectively, if all nucleons are participants. In the case of incomplete stopping, $vQ_{1i}(vQ_{2i})$ is replaced by $\Delta j_{1i}(\Delta j_{2i})$.

V. RELATIVISTIC $n+n$ COLLISIONS

If the collision energy is low, nucleon + nucleon scattering is elastic or excitation, such as $N+N\to N+\Delta$. However, when the collision energy is extremely large, two colliding nucleons pass through each other, and only part of the energy and electromagnetic current are released, which produces both charged and neutral particles. Since wounded nucleons go straight even after collision and each nucleon has a finite size, we can approximate the process as one-dimensional stopping or the deceleration of electromagnetic currents, as in the previous section.

For two reasons, it is hard to know how much electromagnetic current is stopped in high-energy nucleon-nucleon collisions. First, it is experimentally challenging to measure particles in very large rapidity regions. Second, the charge stopping is not well defined in the collision of equal-charged particles such as $p+p$ collisions, since the total electromagnetic current of the system is zero.

We use the PYTHIA event generator to solve the first problem [9]. The upper panel of Fig. 4 shows the electric charge distribution as a function of $\gamma_z\beta_z=\beta_z/\sqrt{1-\beta_z^2}$ in $p+n$ collisions at $\sqrt{s}=200$ GeV from the PYTHIA event generator, where protons move in the $+z$ direction and neutrons in the opposite. Electromagnetic current after the collision is $0.85\,e$ on average, and we thus take $\Delta j=-0.15e$. The middle panel shows bremsstrahlung photon spectra for different stopping times in $p+n$ collisions by using Eqs. (63) and (67), assuming a pointlike particle or a group of valence quarks for the nucleon. We note that the impact parameter in the two equations does not affect the spectrum in $p+n$ collisions, since $Q_2=0$. In both cases, the photon spectrum becomes soft with increasing stopping or deceleration time, while the spectrum at low ω does not change, which is consistent with Fig. 2. We can see that the photon spectrum is larger at high ω in the case of three valence quarks compared to that for a pointlike nucleon. If the neutron is a pointlike particle, it cannot emit photons, while three valence quarks of it (udd) can emit photons in spite of interference, which is completely destructive at low ω but becomes incoherent at high ω, as shown in Fig. 3. That is the reason for the enhancement of photon spectra at high ω in the case of three valence quarks.

In $p+p$ collisions, total electromagnetic current vanishes. Furthermore, it is not clear whether a charged particle produced in the collision is originated from the target proton or from the projectile proton. We assume that the same amount of electromagnetic current is stopped in $p+n$ and $p+p$ collisions. The lower panel of Fig. 4 shows the photon spectra at midrapidity in $p+p$ collisions at $\sqrt{s}=200$ GeV, assuming pointlike nucleons or two groups of three valence quarks. Considering the inelastic scattering cross section of 42 mb, the impact parameter for minimum-bias events is about 0.8 fm on average. As in $p+n$ collisions, the spectrum of bremsstrahlung becomes soft with increasing stopping or deceleration time, while the spectrum at low ω does not change. Since the proton has the same contribution whether it is a pointlike particle or a group of three valence quarks, as shown in Fig. 3, two different pictures bring about similar photon spectra except for the fluctuations, which are ascribed to the interference of photons from the target and projectile protons. The fluctuations are more prominent in the case of pointlike protons.

Here we point out that the spectrum of bremsstrahlung photon at low energy in $p+p$ collisions is not identical to that in $p+n$ collisions. In the limit $\omega\to 0$, Eq. (67) turns to

$$\lim_{\omega\to 0}\frac{dN}{d^2k_T dy}\bigg|_{y=0} = \frac{1}{16\pi^3}\frac{(\Delta v)^2}{\omega^2}\bigg[(Q_1-Q_2)^2 + w^2Q_1Q_2b^2\cos^2\phi - \frac{1}{5}w^2R^2\bigg\{(Q_1-Q_2)^2-\sum_i(Q_{1i}^2+Q_{2i}^2)\bigg\}\bigg], \quad (68)$$

where $\Delta v=\Delta j/Q$ and $R=0$ for the collision of pointlike nucleons. It diverges in $p+n$ collisions ($Q_1=e$, $Q_2=0$), while it has a finite value in $p+p$ collisions ($Q_1=e$, $Q_2=e$):

$$\lim_{\omega\to 0}\frac{dN}{d^2k_T dy}\bigg|_{y=0} = \frac{\alpha(\Delta v)^2}{4\pi^2}\left(\frac{b^2}{2}+\frac{2}{5}R^2\right), \quad (69)$$

where the ensemble average $\langle\cos^2\phi\rangle=1/2$ is taken. The divergence disappears in $p+p$ collisions, because two divergences from each proton stopping cancel each other. However, if the stopping of electromagnetic currents is not symmetric in $p+p$ collisions, the bremsstrahlung photon spectrum diverges at $\omega=0$.

Because of the differences in low-energy photons, it is not right to scale photon spectrum in $p+p$ collisions by the total number of binary collisions to extract nuclear matter effect in heavy-ion collisions, but the number of binary collisions should be separated into the number of $p+p$ collisions, that of $p+n$ collisions, and that of $n+n$ collisions and scaled respectively.

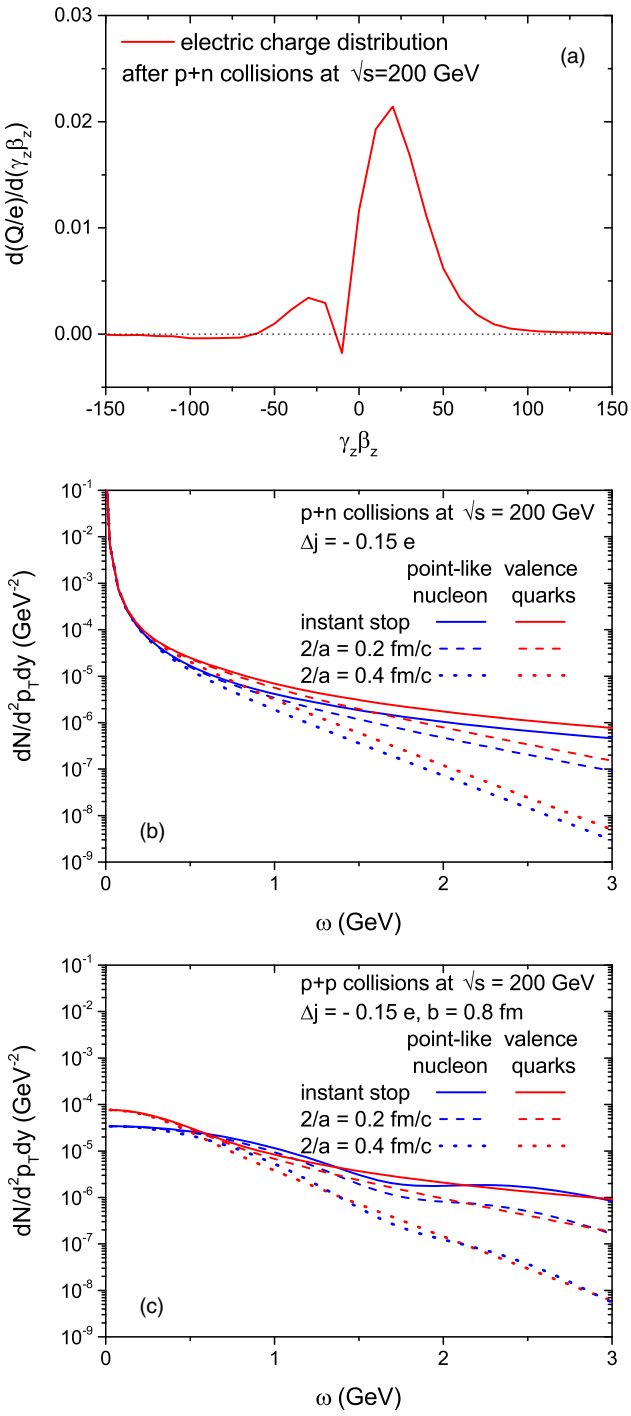

FIG. 4. (a) Electric charge distribution as a function of $\gamma_z\beta_z=\beta_z/\sqrt{1-\beta_z^2}$ in $p+n$ collisions at $\sqrt{s}=200$ GeV from the PYTHIA event generator, and photon spectra for different stopping times in (b) $p+n$ and (c) $p+p$ collisions at the same collision energy, assuming a pointlike particle or a group of valence quarks for the nucleon.

The impact parameter in Eqs. (62) and (67) does not necessarily mean the geometric impact parameter but an

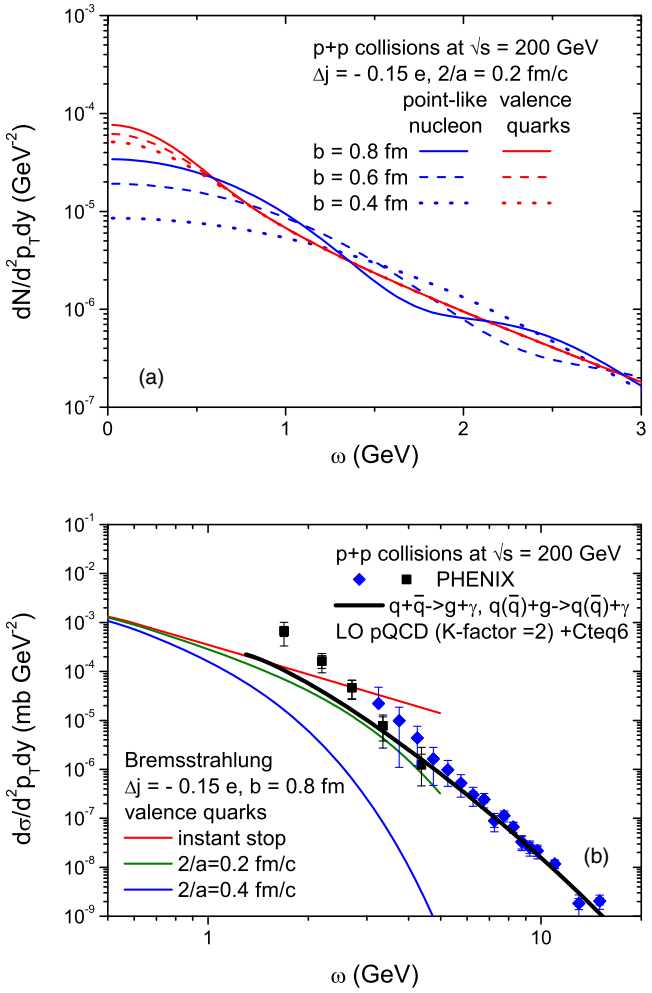

FIG. 5. (a) Spectra of bremsstrahlung photons at midrapidity in $p+p$ collisions at $\sqrt{s}=200$ GeV for the stopping time of 0.2 fm/c and a couple of separation distances. (b) Spectra for $b=0.8$ fm and a couple of stopping times in comparison with the experimental data on direct photons from the PHENIX Collaboration [10,11], along with pQCD calculations.

effective distance between stopped charges of two colliding protons. Since it will be smaller than the geometric impact parameter, we try not only with 0.8 fm but also with smaller values in the upper panel of Fig. 5. The figure shows that the photon spectrum is not sensitive to the separation distance, especially in the case of three valence quarks, where little differences are seen only below $\omega=0.5$ GeV.

The lower panel shows the experimental data on direct photons in $p+p$ collisions at $\sqrt{s}=200$ GeV from the PHENIX Collaboration [10,11], which are compared with pQCD calculations to the leading order for $q+\bar{q}\to g+\gamma$ and $q(\bar{q})+g\to q(\bar{q})+\gamma$ [12] with the CTEQ parton distribution function [13]. The scale of parton distribution function is set at photon energy, and the K factor, which takes into account higher-order corrections, is taken to be 2. We can see that the pQCD calculations reproduce the experimental data down to $\omega=3$–4 GeV and then deviate from them at lower photon energy. Since the calculations are not reliable at low photon energy, they are shown only down to $\omega=1.3$ GeV in the figure.

We also show the bremsstrahlung photons for $b=0.8$ fm and 0, 0.2, and 0.4 fm/c of the stopping time in Eq. (67). Though the comparison with the experimental data cannot say something definite, it seems that the deceleration of electromagnetic current in $p+p$ collisions does not take place instantly but takes a time longer than 0.2 fm/c.

Naively thinking, the deceleration time would be the duration when two nucleons pass through each other. Considering Lorentz contraction, it is only a couple of hundredths of fm/c. However, rich interactions are still left after that—for example, string fragmentation, particle production, and so on. Though the deceleration of electromagnetic currents in $p+p$ collisions may not follow the pattern of Fig. 1, it would be possible to estimate the deceleration time from the bremsstrahlung photon spectrum.

VI. SUMMARY

Relativistic heavy-ion collisions produce hot, dense nuclear matter. The photon is a clear probe for the properties of nuclear matter, because it hardly interacts after production. Since photons are produced from the initial stage to the final one in heavy-ion collisions, they need to be classified according to when they are produced.

At first, nucleons composing nuclei lose considerable energy and momentum through their primary collisions, which bring about the radiation of photons. In the microscopic picture, photons are produced through the scattering of partons in nucleons. The collision of heavy nuclei produces extremely hot nuclear matter, and the matter cools down by emitting thermal photons. Finally, the matter freezes out as noninteracting hadrons, which produce photons through electromagnetic decay. The photons, excluding the last case are called "direct photons."

Nucleon + nucleon collision is a reference experiment to extract nuclear matter effects from heavy-ion collisions, because it hardly produces sizeable matter. Since nucleon + nucleon collisions do not produce thermal photons, all photons excluding those from electromagnetic decay are direct photons, which are produced mostly in the initial stage of collisions. The production of direct photons can be described by parton interactions in pQCD combined with the parton distribution function, if the photon energy is large enough. However, pQCD does not work for low-energy photons.

In this Letter, we have studied the production of bremsstrahlung photons in relativistic nucleon + nucleon collisions, which is not restricted to high-energy photons but is applicable also to low-energy ones. Since the nucleon is not an elementary particle but a composite particle with structure, the stopping of electromagnetic current is modeled by a hyperbolic tangent function with a parameter for stopping time. We also approximate the collisions to

one-dimensional stopping of electromagnetic currents, because two nucleons pass through each other in high-energy collisions. In general, it is hard to measure the amount of stopped electromagnetic current in collisions, because the entire range of rapidity should be covered by detectors. Therefore, we use the PYTHIA event generator and have found that about 15% of initial electromagnetic current stops in $p+n$ collisions at $\sqrt{s}=200$ GeV. The same amount of stopping is assumed in $p+p$ collisions.

We have found that the bremsstrahlung photon spectrum at low energy does not depend on stopping or deceleration time, but only on the amount of stopped electromagnetic current, because low-energy photons cannot provide the information of a short timescale. Beyond this energy range, however, the spectrum becomes soft with increasing stopping time.

We have also studied the effect of nucleon structure by substituting three comoving valence quarks for a pointlike nucleon. In $p+n$ collisions, the substitution enhances the photon spectrum at large energy, because neutrons cannot emit photons, while three valence quarks composing the neutron can emit photons, and each photon becomes incoherent as photon energy increases. In $p+p$ collisions, bremsstrahlung photons can be emitted from both the projectile and target protons, and interference could be destructive or constructive. For example, if the impact parameter in $p+p$ collision vanishes, the interference is completely destructive, and no bremsstrahlung photon is produced. In the picture of comoving valence quarks, however, the fluctuations of the bremsstrahlung photon spectrum caused by the interference reduce, and the photon does not vanish even at $b=0$.

The photon spectrum in $p+n$ collisions and that in $p+p$ collisions are quite different from each other at low energy, and we suggest that the photon spectrum in $p+p$ collisions should not be rescaled simply by the number of binary collisions in heavy-ion collisions, when the nuclear matter effect is studied, but by the number of binary $p+p$ collisions, that of $p+n$ collisions, and that of $n+n$ collisions counted separately.

Comparing the bremsstrahlung photon spectrum with the experimental data on direct photons from the PHENIX Collaboration, it seems that the stopping of electromagnetic current in relativistic $p+p$ collisions does not take place instantly but takes a time, which is longer than the overlapping time of two nucleons, because there are additional processes, such as particle production.

ACKNOWLEDGMENTS

The authors acknowledge inspiring discussions with W. Cassing and E. Bratkovskaya. This work was supported by the LOEWE center HIC for FAIR, the HGS-HIRe for FAIR and the COST Action THOR, No. CA15213. Furthermore, P. M. and E. B. acknowledge support by DFG through Grant No. CRC-TR 211, "Strong-interaction matter under extreme conditions." The computational resources have been provided by the LOEWE-CSC.

APPENDIX: FOURIER TRANSFORMATIONS

In this Appendix, we show the Fourier transformation of basic functions.

1. Signum function

The signum function is defined as

$$\begin{aligned}\mathrm{sgn}(t) &= 1(t\geq 0),\\ &= -1(t<0).\end{aligned} \tag{A1}$$

It can be expressed as

$$\mathrm{sgn}(t)=\lim_{a\to 0^+}\{e^{-at}\theta(t)-e^{at}\theta(-t)\}, \tag{A2}$$

where $\theta(t)$ is the step function, and the Fourier transformation of the signum function is derived as given below:

$$\begin{aligned}F_w[\mathrm{sgn}(t)] &= \lim_{a\to 0^+}\left(\int_0^\infty e^{-at}e^{-iwt}dt-\int_{-\infty}^0 e^{at}e^{-iwt}dt\right)\\ &= \lim_{a\to 0^+}\left(\frac{1}{a+iw}-\frac{1}{a-iw}\right)=\frac{2}{iw}.\end{aligned} \tag{A3}$$

2. Step function

The step function is expressed by using the signum function

$$\theta(t)=\frac{1}{2}\{1+\mathrm{sgn}(t)\}, \tag{A4}$$

and after Fourier transformation,

$$F_w[\theta(t)]=\frac{1}{2}\{F_w[1]+F_w[\mathrm{sgn}(t)]\}=\pi\delta(w)+\frac{1}{iw}. \tag{A5}$$

3. Box function

Supposing the box function is centered at $t=0$ with the width T:

$$\begin{aligned}\mathrm{rect}_T(t) &= 1, \quad \text{if } |t|\leq T/2,\\ \mathrm{rect}_T(t) &= 0, \quad \text{if } |t|>0,\end{aligned} \tag{A6}$$

then the Fourier transformation is carried out as follows:

$$\begin{aligned}\int \mathrm{rect}_T(t)e^{-iwt}dt &= \int_{-T/2}^{T/2}e^{-iwt}dt=\frac{i}{w}(e^{-iwT/2}-e^{iwT/2})\\ &= \frac{2\sin(wT/2)}{w}.\end{aligned} \tag{A7}$$

4. Hyperbolic tangent

The Fourier transformation of the hyperbolic tangent is given by

$$F_w[\tanh(t)] = -i\pi \operatorname{csch}\left(\frac{\pi w}{2}\right), \tag{A8}$$

from which

$$F_w[\tanh(at)] = \int dt \tanh(at) e^{-wt} = \frac{1}{a}\int d(at) \tanh(at) e^{-\frac{w}{a}at} = -i\frac{\pi}{a}\operatorname{csch}\left(\frac{\pi w}{2a}\right). \tag{A9}$$

Eq. (A3) is easily proved from Eq. (A9) as follows:

$$F_w[\operatorname{sgn}(t)] = \lim_{a\to\infty} F_w[\tanh(at)] = \lim_{a\to\infty} \frac{\pi}{ai}\operatorname{csch}\left(\frac{\pi w}{2a}\right) = \lim_{a\to\infty} \frac{\pi}{ai}\frac{2}{\exp(\frac{\pi w}{2a}) - \exp(-\frac{\pi w}{2a})} = \frac{2}{iw}. \tag{A10}$$

[1] A. Adare *et al.* (PHENIX Collaboration), Phys. Rev. C **91**, 064904 (2015).
[2] V. Koch, B. Blttel, W. Cassing, and U. Mosel, Phys. Lett. B **236**, 135 (1990).
[3] C. Itzykson and J. B. Zuber, *Quantum Field Theory* (McGraw-Hill, New York, 1980).
[4] T. S. Bir, Z. Szendi, and Z. Schram, Eur. Phys. J. A **50**, 60 (2014).
[5] K. Haglin, C. Gale, and V. Emel'yamnov, Phys. Rev. D **47**, 973 (1993).
[6] H. C. Eggers, R. Tabti, C. Gale, and K. Haglin, Phys. Rev. D **53**, 4822 (1996).
[7] J. Cleymans, V. V. Goloviznin, and K. Redlich, Phys. Rev. D **47**, 173 (1993).
[8] T. Koide and T. Kodama, J. Phys. G **43**, 095103 (2016).
[9] T. Sjostrand, S. Mrenna, and P. Z. Skands, J. High Energy Phys. 05 (2006) 026.
[10] S. S. Adler *et al.* (PHENIX Collaboration), Phys. Rev. Lett. **98**, 012002 (2007).
[11] A. Adare *et al.* (PHENIX Collaboration), Phys. Rev. Lett. **104**, 132301 (2010).
[12] C. Y. Wong and H. Wang, Phys. Rev. C **58**, 376 (1998).
[13] J. Pumplin, D. R. Stump, J. Huston, H. L. Lai, P. M. Nadolsky, and W. K. Tung, J. High Energy Phys. 07 (2002) 012.